International Communications in Heat and Mass Transfer 118 (2020) 104901

Contents lists available at ScienceDirect

International Communications in Heat and Mass Transfer

journal homepage: www.elsevier.com/locate/ichmt

# Experimental investigation on the ice melting heat transfer with a steam jet impingement method

Wen-Tao Ji[a,*], Xiao-Dong Lu[a], Li Chen[a], Yi-Wei Zhang[b], Wen-Quan Tao[a]

[a] Key Laboratory of Thermo-Fluid Science and Engineering of MOE, School of Energy and Power Engineering, Xi'an Jiaotong University, Xi'an 710049, Shaanxi, China
[b] Qujing Power Supply Bureau, Yunnan Power Supply Company, Ltd, Qujing 655000, Yunnan, China

ARTICLE INFO

*Keywords:*
Jet impingement
Heat transfer
Ice removal
Steam

ABSTRACT

In winter, ice is the common adhesive along many outdoor facilities. It has severe impacts on human activities. In this study, jet impingement of high velocity steam on ice surface was investigated with an experimental approach. In the experiment, the temperature of steam was approximately 140 °C. Non-dimensional nozzle-to-ice spacing (initial nozzle-to-ice distance over the diameter of nozzle) ranged from 5 to 18. The steam was supplied at a steady state. The effects of non-dimensional nozzle-to-ice spacing, nozzle exit velocity, nozzle number, and nozzle diameter on heat and mass transfer were tested. From the experimental results, it is recommended that the dimensionless distance for nozzle to ice should be controlled within 12. The largest energy efficiency and the best ice melting rate appeared at nozzle exit steam velocity of 40 m/s, not the highest nozzle exit velocity in the measurement. For the nozzles with one single pipe and two pipes with same external diameter, at lower distance, one pipe nozzle has higher heat transfer performance. The effect of nozzle diameter on heat transfer was negligible for the four nozzle types in the experiment. The experiment data should have a guiding significance for the design of high-efficiency instruments for ice removal.

## 1. Introduction

In winter, ice is the common adhesive along electric power lines, aircraft wings, wind turbine blades, outdoor switches, and many other facilities. Adhesion of ice outside these surfaces have caused large impacts on human daily life and industrial production. However, these related problems have still not been well resolved so far. It is still difficult to separate ice from the internal structure. One of the solutions is heating, through air [1–3], steam [4–6], hot water [7–9], radiation [10–13]. Most of the studies on ice removal or melting are through experimental approaches. Analytical and numerical methods are also adopted [14–17]. The related researches on the ice removal methods are briefly summed up as follows.

Koenig and Ryerson [18] experimentally investigated the processes of ice melting for aircrafts with infrared heaters. Ice was removed by remotely located emitters. The melt rate versus the infrared heater temperature, and the most effective infrared wavelengths were obtained. To obtain more of the infrared energy in the visible wavelengths, it required a higher heater operating temperature. The mechanisms, transmission of radiant energy, were investigated. In the experiment, the heater was 4 m away from the ice surface. The testing indicates that ice can absorb most of emitted radiance between wavelength of 0.4 and 20 μm effectively. Very small amount of energy is transmitted through the ice for wavelengths greater than 3 μm, even for ice as thin as 1 mm. This method is not suitable for the places with higher altitude or that far away from power supply. In order to provide sufficient radiation heat exchange area, the drawback is that the infrared heater is normally very large.

Xie et al. [19] investigated the deicing features with hot air. In experiment, ice was frozen outside an aluminum plate. The thicknesses of ice in the investigation were 2.0 and 5.0 cm. The distance of ice and hot air tuyere was 40 cm. Melting rate, mass, temperature at different positions, deicing time were studied under different test conditions. The temperature of hot air was in the range of 30 to 60 °C and the velocity ranged from 5 to 14 m/s. They found that the advantageous temperature was 40–50 °C,not the highest temperature, 60 °C. The favorable velocity of hot air was 8–14 m/s. The maximum energy efficiency of deicing was 12.1%. This method is comparably less efficient, because lots of heat was dissipated into the atmosphere.

Hot water is also used for ice melting (Burnett et al. [20], Blythe et al. [21], Rack et al. [22], Makinson et al. [24], Liu et al. [25], and Talalay et al. [26]). In the experiment, hot water is pressured and delivered to ice surface through high pressure pump and hose. It can be used for melting ice or drilling the deep ice up to 2500 m. The key

* Corresponding author.
*E-mail address:* wentaoji@xjtu.edu.cn (W.-T. Ji).

https://doi.org/10.1016/j.icheatmasstransfer.2020.104901

Available online 03 October 2020
0735-1933/ 

parameters for melting process include the water temperature, flow rate and pressure. The temperature of water is normally in the range of 60–90 °C and flow rate of 10 to 200 L/min. The energy of boiler can be provided by diesel fuel. Different types of nozzles are used as the requirements on water jet strength, drilling speed and diameters of borehole are different. Combined with the melt water, a large number of water would flow out from the ice melting cavity. Seed water can be firstly obtained from the local ice or snow. The admixture of melt water and heating water can also be recovered, filtered, and reused.

Resistive heater is also used directly for ice melting. In the study of Talalay et al. [27], the heated head was a coiled tubular heating element cast integrally with copper annulus. Ice melted around the heated head. In order to make the ice melting quickly, the power density of electric heater can provide the heat flux of at least $1 \times 10^6$ W/m$^2$. The coiled shape thermal head had the external diameter of 135 mm and internal diameter of 110 mm, respectively. The axial load applied vertically on the thermal head can minimize the heat loss to the melt water, because melt water can be squeezed out from the thermal head and ice surface. The disadvantages of electrical heating method are that it needs a higher power supply, and the efficiency will decrease when the heater cannot contact with ice surface. The protective measures will be necessary for electrical insulation of high-capacity long-distance transmission lines.

Impingement of high-pressure steam jet can also be used for ice removal. It is particularly helpful for the ice removal from key components of outdoor facilities. Using the steam jet to heat ice is advantageous for many reasons. No pumps and power supply are required. Small and portable equipment can be designed. Hodge [5] investigated the drill rates of a steam-operated ice drill. In the study, high temperature steam was transmitted to the ice surface via a double-layered flexible hose. The outer layer of the hose is rubber and the internal is made by Teflon. The facility was used to drill holes in the glacier and sea ice. The depth and diameter of the drilled hole were measured in the experiment. When the ice drill was used under arctic conditions, the major problem encountered was the heat loss of hose to environment. The heat loss by hose at different distance for various lengths of hose was also calculated while the temperature of steam was 141 ° C. Masuda et al. [28] experimentally tested the impingement of high-pressure steam jet on the flat plate. The nozzles had the shape of circles and ellipses. Experimental results indicated that the value of thrust coefficient for circular nozzle with round edge was basically 1.24 times of Moody's value [29]. But the value for other types was smaller than 1.24. For both circular and elliptical nozzles, the variation of pressure distribution as the function of impingement distance was similar. The heat transfer coefficient of ice melting for steam condensation is about 100 times higher than that by dry hot air [30]. A model for steam condensation was developed by Woodcock et al. [31]. According to the analysis, the heat transfer rates of steam condensation outside the ice surface can reach up to 1 MWm$^{-2}$. When the free convection of steam was changed into forced convection, the heat flux can reach up to 2 MWm$^{-2}$. When the cavity was filled with water, the heat transfer coefficient was an order of magnitude lower than that without water.

The common methods for deicing include mechanical method, hot water, hot air, electrical thermal resistance, and infrared radiation. These methods have their own advantages and disadvantages. For mechanical method, electricity must be provided, and it usually cannot be operated remotely. Infrared radiation has a very high heat source temperature, up to thousands of degrees Celsius. When the ice thickness on the surface of the equipment is very thin, especially less than 1 mm. The infrared radiation deicing method is likely to damage the surface of the equipment which may lead to security issues. For hot-water method, the water consumption is very large, electricity power should be provided for pumps, and the temperature of water cannot reach very high temperatures, mostly within 100 °C. The energy required for hot-water drill is also much larger than the energy required for a mechanical ice drill. For the steam jet impingement method, it can be used for drilling up to 12 m long. When steam is ejected from the nozzle and contacts the ice surface, the steam transfers its energy to the ice. The latent heat for evaporation ensures a very efficient energy flow from the boiler to the nozzle. When it is used for deicing and drilling, only fuel for the boiler and water to generate steam are required. It makes the steam-driven deicing method to be lighter weight and lower cost. While, most of experimental researches for steam deicing mainly focused on measuring the depth of the hole and the weight of the ice drill system.

Normally, heat transfer and flow characteristic of steam jet impingement are influenced by the following factors: steam velocity, fluid thermal properties, nozzle geometry, nozzle-to-surface spacing, and the angle between nozzle axis and jet wall. Moreover, dissipation of heat inside the ice and the surrounding environment also has effects on the heat transfer. Removal of ice with the steam jet condensation method is still insufficient. Related literature reported the design of boiler, insulated hose distance, and capacity of ice removal. Details from the prospective of heat transfer, energy efficiency, vapor temperature, vapor velocity, and different types of nozzles were rarely provided. In nowadays, freezing rain, extreme cold weather, and severe environments still continues to occur in winter. Many facilities could be frozen or form a layer of ice adhering to the substrate. It can have severe impacts on human activities. In order to adequately prepare for these extreme weather, minimize its potential adverse impact, and develop the equipment for ice melting of outdoor facility, there is a need for a more detailed study and better understanding the mechanisms of ice melting with the above mentioned steam jet impingement method from the perspective of heat transfer. The present work is conducted to qualitatively measure the jet impingement heat transfer of steam and ice with an experimental approach. The performance of steam jet impingement on melting ice was evaluated, and the effects of steam nozzle exit velocity, nozzle diameter, initial distance between nozzle exit and ice surface, number of nozzles, and jet time on the heat transfer were also analyzed. The experiment data should have a guiding significance for the design of high-efficiency instruments for ice removal.

## 2. Experimental apparatus

The schematic of the used experimental apparatus is shown in Fig. 1(a). Main parts of the experimental apparatus include: steam generation, power regulation, data acquisition, and targeted ice surface. The schematic of nozzle to vertically targeted ice surface is shown in Fig. 1(b). The container for ice with the shape of a truncated cone has a top inner diameter 245 mm, bottom inner diameter of 180 mm, and height of 225 mm, respectively. To prevent heat transfer between ice and surrounding environment, the container of ice was wrapped with rubber plastic insulating material with a thickness of 50 mm. In addition, a thin layer of aluminum foil with a thickness of 1 mm was used to wrap the outer surface of insulating material to prevent heat radiation. In the experiment, the axis of ice container was in a direction perpendicular to the direction of gravity. Melt water and steam condensate can fully drain out from the steam jet impinging cavity (Fig. 1(b)).

The steam boiler is a pressure vessel made by 304 stainless steel. It has an inner diameter of 30 cm and is 50.5 cm in height. The thickness of the vessel wall is 6 mm. The vessel can hold 20 kg of water for each experiment. The external of pressure vessel is also wrapped with rubber material and aluminum foil for insulation. It also has a sight glass to monitor the water level in the vessel. During the experiment, liquid water in the vessel is vaporized through an electric heating method. The power of the electrical heater can be adjusted by a power regulator in the range of 0 to 4 kW. Water should firstly be heated to the boiling point. Two electric heating rods with the length of 150 mm are installed at the bottom of the boiler. Different outlet vapor velocities are corresponding to different electric heating powers. The pressure in the vessel is measured by a pressure gauge with a precision of ± 0.01%. The temperature of liquid water and steam can be measured by a platinum

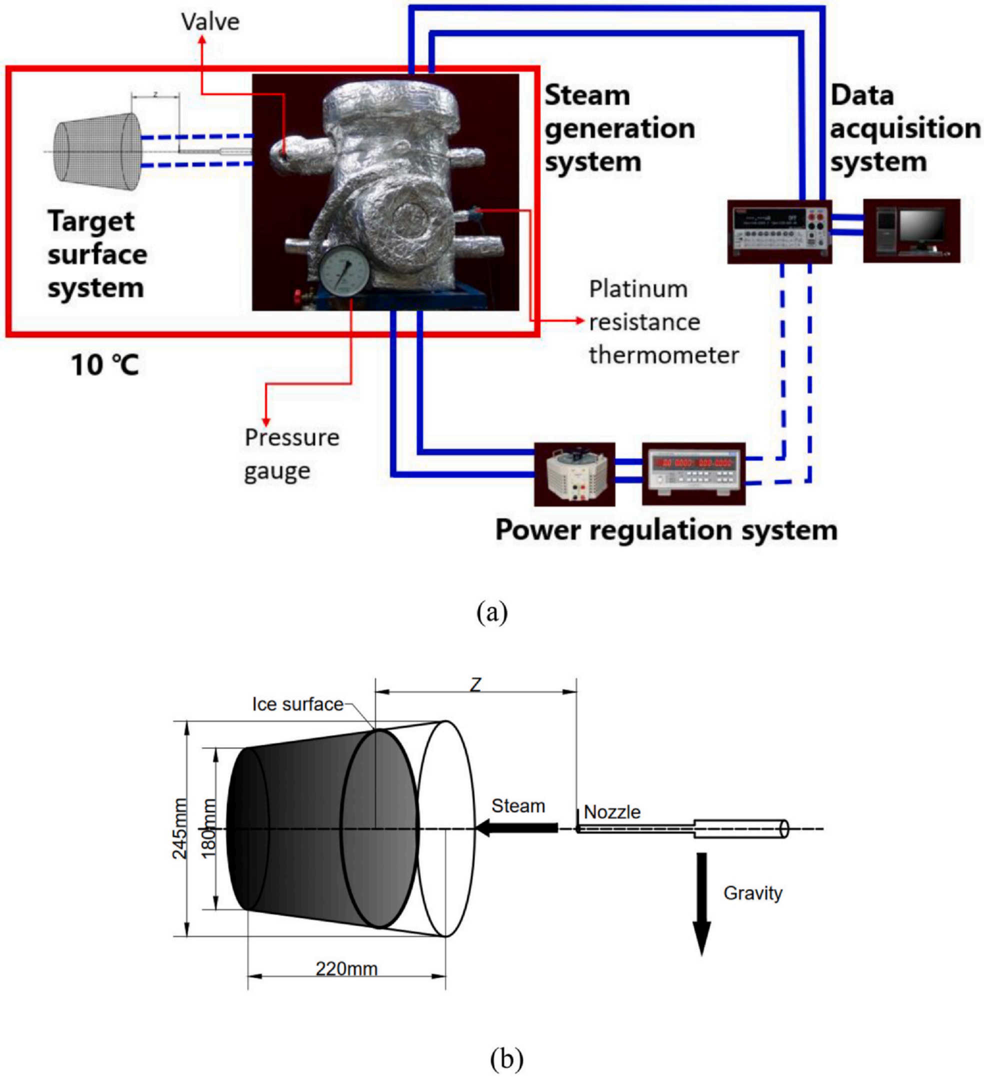


**Fig. 1.** Schematic diagram of the experimental system and nozzle to target surface.

resistance thermometer with an accuracy of ± 0.05 K. The temperature of ice is measured by copper-constantan thermocouples, which are calibrated against a platinum resistance thermometer with the precision of ± 0.05 K. The thermocouples are mounted inside the ice before freezing. A Keithley 2700 digital voltmeter is used for data collection. The steam jet is impinged to the ice surface and the ice container is placed opposite to the nozzle. The angle between nozzle axis and initial ice surface is 90°. The position of ice container can be adjusted according to the requirements of experiment. The velocity of the jet steam is measured by an anemometer with a precision of 0.1 m/s at different nozzle-to-ice spacing along the axis of the nozzle. The nominal steam jet impinging velocity (30 m/s, 40 m/s and 50 m/s) is tested at the exit of nozzle. Impinging velocity to the ice surface is also measured. In such cases, the probe is placed at the location where the ice surface will be positioned. The velocity of the steam is the average value of five measurements at the intervals of 5 min. Each measurement is the average value for 30 s. The jet velocity can be adjusted through the valve at the outlet of the nozzle. The initial mass of water in the container of ice is approximately 6.5 kg, which is measured by an electronic scale with precision of ± 0.1 g. During the experiment, room temperature is maintained at 10 °C, atmospheric pressure is about 0.097 MPa, and average relative humidity is about 50%. As the environmental condition does not change throughout the experiment, the impact of environmental changes on the experimental measurements can be ignored.

In the experiment, the nozzle is of a pipe-type. Four different types of pipes are used. Some of the pipe-type nozzles have an outer diameter of 8 mm and a thickness of 1 mm. Other nozzles have an external diameter of 12 mm, 16 mm, 19 mm and thickness of 1 mm. The spacing of jet-to-jet is 8 mm when using multiple jets. The length of the pipe-type nozzle is 130 ± 5 mm. Photo and schematic of pipe-type nozzles used in the experiment are shown in Fig. 2. The ice surface before the experiment is shown in Fig. 3(a). The ice surface at different initial nozzle exit-to-ice surface spacing during the experiment is shown in Fig. 3(b). Before the experiment, tap water is charged into the ice container. The thermocouples are also submerged in the water. The level of water should be at least 20 mm below the rim. Then the containers for ice are moved to the refrigerator. The temperature of refrigerator is maintained at about −15 °C. After about two days, the ice container can be taken out for experiment. The density of ice in the experiment is about 916 kg/m$^3$ at 0 °C.

## 3. Experimental procedures

Before the experiment, the tightness of the steam boiler should be check. High pressure nitrogen of 1.5 MPa is charged into the boiler. The high pressure should not change over 24 h. If no leakage is detected, water is pumped into the boiler by a pressure pump. The level of water

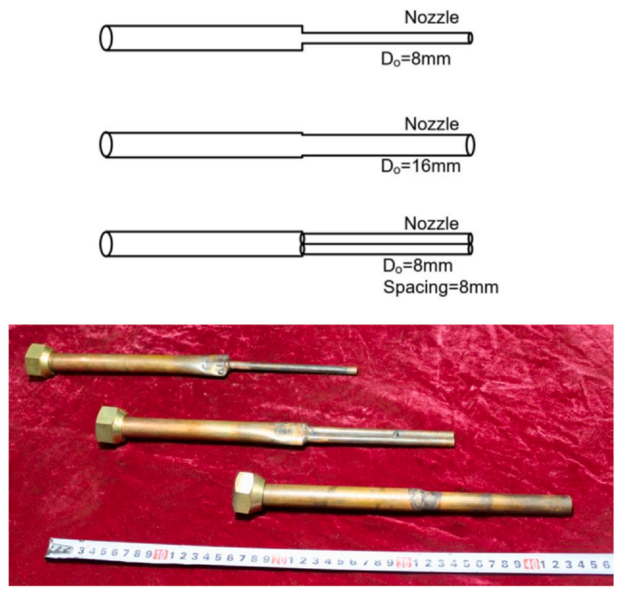


**Fig. 2.** Schematic diagram and photo of the pipe-type nozzles.

in the boiler should not exceed the nozzle exit. Water charged into the vessel should be at least 20 kg. Then the water in the boiler is heated by electric heating rods. The vapor exit valve should be closed during this process. When the water temperature reached a certain saturation temperature, the vapor exit valve can be opened and high pressure saturated steam is ejected through the pipe-type nozzle. The valve at the nozzle exit and the power regulator can be used to adjust and obtain the required stable jet flow rates. The experimental system has been heated and operated stably for 3 h before the experiment.

Before the data acquisition, the steam jet impingement should be in a steady state. This should be tested with the steam velocity meter. The steady state in the experiment is featured by: (1) the temperature difference between liquid water in the boiler and steam is within ± 0.5 K; (2) the temperature fluctuation of liquid water and steam is within ± 0.5 K; (3) the velocity fluctuation of the steam is within ± 0.5 m/s at the same location. The mass of ice (included in the container), $m_1$, is weighed with an electrical scale before the experiment. Then the container for ice is placed in a fixed position. The nozzle is moved to the opposite side of the ice container. The distance between ice surface and nozzle exit is measured and the position of the ice is adjusted to obtain the required distance. Then, the steam jet begins to impinging on the target surface. Meanwhile, the data acquisition system starts to collect the experimental data. The jet impinging time for each experiment is adjusted according to the purpose of the experiment. In the experiment, the distance between ice container and nozzle exit is fixed. As the experiment progresses, the distance between ice melting surface and nozzle exit increases. Melt water leaves the ice container by gravity. After the jet impingement, the ice container is weighed immediately to obtain $m_2$. Ice bucket should be drained prior to each weighting. The difference of mass, $m_1 - m_2$, is the mass of melting. And the procedures of acquiring data and weighing are repeated several times to obtain the experimental data at different conditions.

## 4. Data reduction and uncertainty analysis

The energy efficiency, power absorbed by ice, and electric heating power are defined by the following equations:

$$\gamma = P_t/P_0 \tag{1}$$

$$P_t = \frac{(m_1 - m_2) \times r}{t} \tag{2}$$

$$P_0 = I^2 \times U \tag{3}$$

where $P_0$ is the electric heating power when the steam boiler is running steadily. And the value can be obtained by three-phase electrical parameter measuring instrument (with accuracy of ± 1 W). $P_t$ is the energy absorbed by melting ice at per second. $\gamma$ is the energy efficiency. $m_1$ and $m_2$ are the mass of ice before and after experiment, respectively. $t$ is the melting time that can be recorded in the experiment. $r$ is the latent heat of ice melting. $I$ and $U$ are heating current and voltage, respectively.

$T_w$ is the initial temperature of ice. The value can be measured by copper-constantan thermocouples. In the experiment, the temperature of ice is very close to 0 °C. $T_{l,\ sat}$ is the saturation temperature of liquid water. $T_{s,\ sat}$ is the temperature of steam. The two temperatures can be measured by the four wire resistance temperature detectors (RTDs). $T_j$ is the jet temperature. As the whole experimental system and pipe line are well insulated, and the length of the connecting pipe is very short, the heat loss should be negligible in the experiment. Therefore, the temperature $T_{s,\ sat}$ can be regarded as the temperature of $T_j$. The steam vaporization and heating process are in thermal equilibrium state. The value of $T_{s,\ sat}$ is set to be 140 ± 0.5 °C in the experiment. The corresponding saturation pressure is 0.3615 ± 0.0051 MPa. This is a typical oil-fired steam boiler working condition.

Uncertainty analysis is conducted using the method proposed by Moffat [35], and the results are summarized in Table 1.

## 5. Results and discussions

In order to design an ice removal device for outdoor facilities, it is required to understand various characteristics of steam impingement jets on ice. In the present investigation, experiments were conducted in order to determine the effects of jet velocity, nozzle-to-surface distance, nozzle geometry and impinging time on the heat transfer. This will be discussed in detail in the following sections.

### 5.1. Effect of nozzle-to-ice distance

Nozzle-to-ice spacing has an important effect on the steam impinging jet flow and heat transfer. Fig. 4(a) shows the variation of ice ablation mass for different nozzle-to-initial ice distance. The melting rate is fast at lower distance and slower for longer distance. As the decrease of jet exit-to-ice surface spacing, the heat transfer intensity should be increased. For the steam impingement on ice, a nonlinear characteristic of melting rate is observed. The difference of mass ($m_2$ - $m_1$) is smaller between $V_o$ = 40 m/s and 50 m/s than that between $V_o$ = 30 m/s and 40 m/s at the same distance, especially that at lower $z/D_o$, where $z$ is the initial nozzle-to-ice surface spacing and $D_o$ is the outer diameter of nozzle pipe(mm). As the nozzle outlet flow velocity decreases, the effect of $z/D_o$ will also decrease. The decreasing of melting rate is larger at lower $z/D_o$. The energy efficiency for 40 m/s is larger. Under identical conditions the vapor velocity of 40 m/s can provide relatively higher efficiency than 50 and 30 m/s. As steam velocity decreases, the high-velocity jet impact should decrease. This nonlinear feature is caused by both the heat transfer of convection, interaction between ice surface and steam, and the changes in the shape of steam-ice contact surface. The original ice contacting surface is flat and gradually changes into concave as the experiment progresses. That's the reason the ice melting rate is decreasing at longer distance. While, as shown in Fig. 4(a), the effect of nozzle exit velocity is less pronounced as the dimensionless nozzle-to-ice spacing($z/D_o$) reaches over 14. The experimental correlation between ice melt mass and initial non-dimensional nozzle-to-ice surface distances are shown as follows:

$$m = 332.91 - 19.51 \times z/D_0 + 0.488 \times (z/D_0)^2 \ (V_o = 30 \text{ m/s}) \tag{4}$$

$$m = 514.11 - 40.58 \times z/D_0 + 1.161 \times (z/D_0)^2 \ (V_o = 40 \text{ m/s}) \tag{5}$$

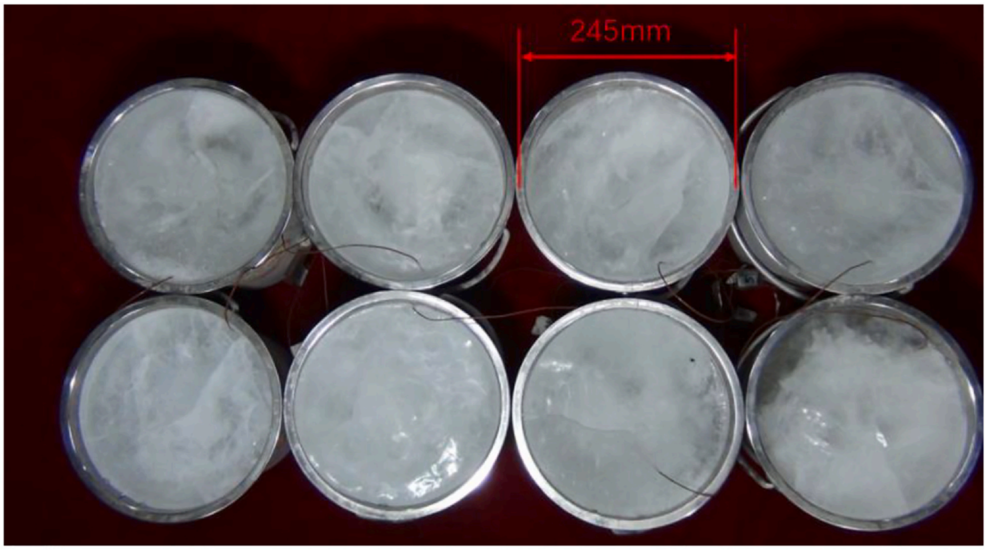


(a)

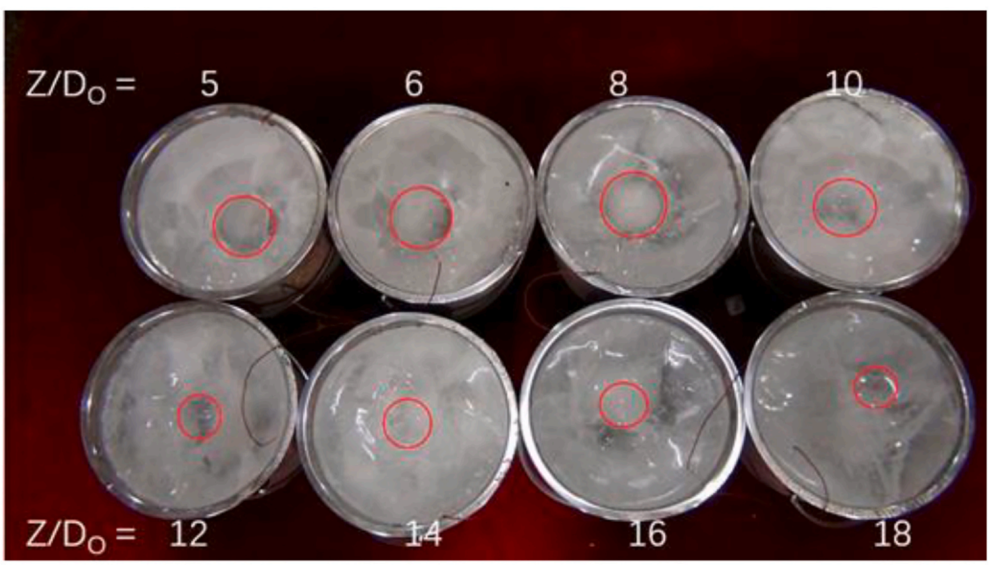


(b)

**Fig. 3.** Ice in experiments.

**Table 1**
Results of n$^{th}$-order uncertainty analysis.

| Resultants | Nominal Value | Nth-order uncertainty (%) | Largest Source |
|---|---|---|---|
| $P_t$ | 306.2(W) | 7.58 | $\Delta m$ |
| $P_0$ | 1180(W) | 1.69 | $I$ |
| $\gamma$ | 0.25 | 7.77 | $P_t$ |
| $V$ | 5.77 (m/s) | 5.01 | $V$ |
| $z/D_0$ | 5 | 0.56 | z |

$$m = 553.08 - 42.88 \times z/D_0 + 1.179 \times (z/D_0)^2\ (V_o = 50\ \text{m/s}) \tag{6}$$

The relative humidity also affects the flow of steam jet. As the air is unsaturated, the average relative humidity is around 50% at air temperature of 10 °C in the experiment. The jet during the passage will release steam to the air. As the increase of the distance between jet exit and ice, more steam would be discharged into the air. Fig. 4(b) shows the distribution of steam velocity at different dimensionless nozzle-to-ice spacing and nozzle exit velocities. The velocity of the steam jet for different distances is tested along the axis of the nozzle. For dimensionless nozzle-to-ice spacing $z/D_o$ ranges from 5 to 18 and nozzle exit velocity in the ranges of 30 m/s to 50 m/s, the steam flow velocity decreases monotonically as the spacing increases. In the experimental test conditions, the velocities are 15.5, 20.8 and 25.1m/s at $z/D_o = 5$ and 5.8, 6.9 and 7.7m/s at $z/D_o = 18$ for the nozzle exit velocity of approximately 30, 40 and 50 m/s, respectively. The difference of velocity is larger at lower spacing than that at larger jet exit-to-ice distances. The velocities are in good agreement with a polynomial fitting formula for $z/D_o$ ranging from 5 to 18. The velocity gradient at the

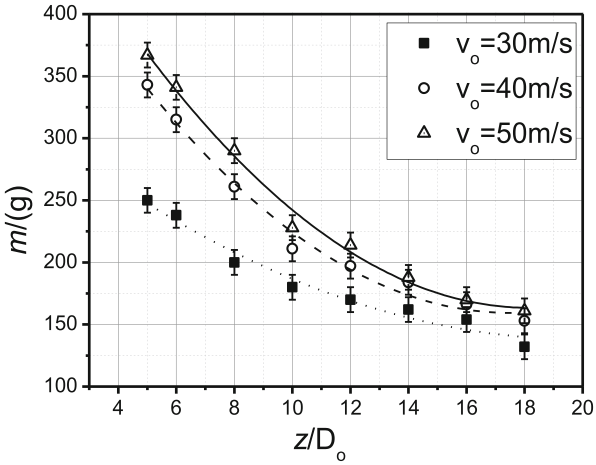


(a)

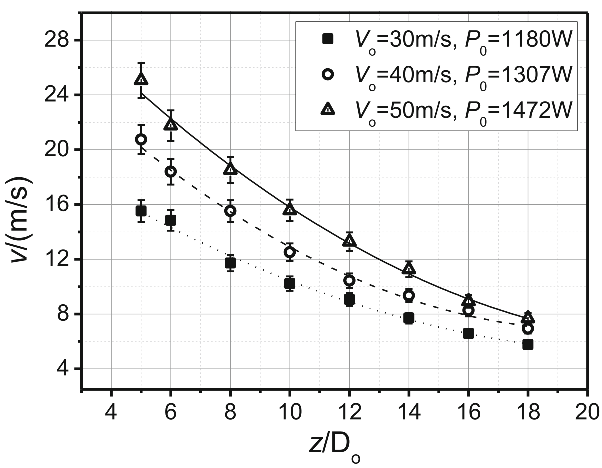


(b)

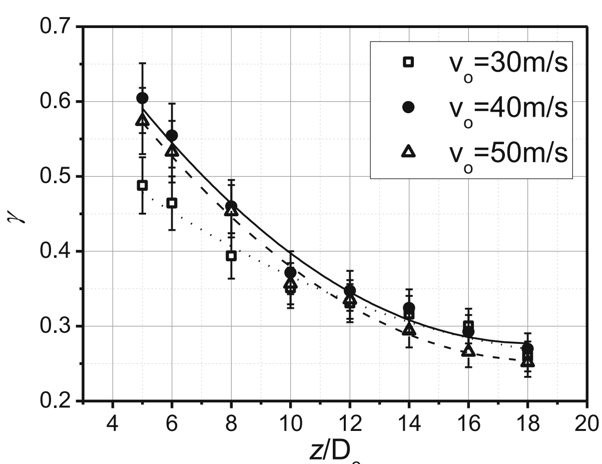


(c)

**Fig. 4.** The effect of dimensionless nozzle-to-ice spacing and nozzle exit velocity.

stagnation line is linearly related to the dimensionless nozzle-to-ice spacing, and the results are in agreement with Stevens and Webb's conclusions [36]. Three correlations for velocity of steam at different location and dimensionless nozzle-to-ice distance are shown as follows:

$$V = 22.65 - 1.60 \times z/D_0 + 0.037 \times (z/D_0)^2\ (V_o = 30\ \text{m/s}) \tag{7}$$

$$V = 31.35 - 2.50 \times z/D_0 + 0.065 \times (z/D_0)^2\ (V_o = 40\ \text{m/s}) \tag{8}$$

$$V = 35.91 - 2.59 \times z/D_0 + 0.057 \times (z/D_0)^2\ (V_o = 50\ \text{m/s}) \tag{9}$$

The relationship shows that the coefficient of the quadratic term for 40 m/s is the largest. It indicates that the effect of $z/D_o$ at nozzle exit velocity of 40 m/s is larger than the other velocities. The release of vapor into atmospheric environment is influenced by many factors, such as velocity of steam, temperature difference, average humidity of air, and air turbulence. The decreasing rate of the steam velocity at different locations is larger for 50 m/s compared with that of 30 m/s. The larger the impingement velocity, the more steam will be released to the air. At the distance of $z/D_o$ equals to 5, the steam velocity at this position is about one half of the nozzle exit steam velocity. For the distance $z/D_o$ larger than 18, only about 15% of the nozzle exit steam velocity are left. If the ice removal devices are used in extreme cold weather, this effect should be more significant. At a larger distance, the difference of steam velocity at different locations is rather small. This indicates that the loss of steam into the atmospheric environment is severe for the steam jet impingement. As the distance of jet exit and ice container is fixed, the actual impinging ice surface is moving backward in the experiment. The distance of nozzle exit and ice surface should be as small as possible to achieve higher heat transfer efficiency. According the analysis above, it is recommended that this distance is controlled within 12 expressed through the dimensionless distance $z/D_o$.

Energy efficiency is another important consideration for the design of an ice removal instrument. Fig. 4(c) shows the energy efficiency at different dimensionless jet exit-to-ice surface spacing. The efficiency is higher at lower distance. It decreases rapidly with an increase of distance. Within the test range, the overall average efficiency is the largest for $V_o = 40$ m/s. In other words, the energy loss is the smallest or the efficiency of energy is the highest for $V_o = 40$ m/s. The nozzle exit velocity of 40 m/s could be selected as jet velocity to save energy. The difference of the ratio is relatively small as $z/D_o$ greater than 10, almost within the uncertainty of experimental data. The reason for the lower efficiency with larger distance at $V_o = 50$ m/s might be that the vapor and heat dissipation is relatively severe to the environment. When the steam reaches the ice surface, the effect of jet impingement will become weaker for the longer distance. The dryer of the ambient air, the more steam would be dissipated to the atmosphere.

### 5.2. Effect of jet time

Fig. 5 shows the mass of melted ice as a function of steam jet impingement time. In this experiment, the container of ice and nozzle exit is kept at a fixed position. The initial dimensionless nozzle-to-ice

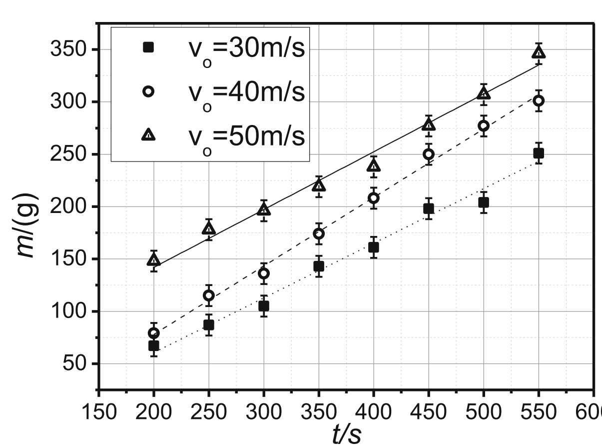


**Fig. 5.** The effect of jet time on ice melting at $z/D_o = 10$.

spacing is 10. As the experiment progresses, the distance of ice surface and nozzle exit will increase and shape of impinging ice surface might change into concave, but the position of most ice left in the container is fixed. Melt-water will flow out from the bottom of the concave. After the experiment, the amount of ice in the container still left is at least 90% of the initial ice content(Fig. 3(b)). The amount of ice in the container is sufficient so that the steam cannot reach the inner wall of the container.

As shown in Fig. 5, at higher nozzle exit velocity, heat and mass transfer rate between steam and target surface is larger, which makes the mass of melted ice also larger at the same location and jet time. As jet time increases, heat and mass transfer between steam and the target surface make the target surface move away from the nozzle exit. The high-velocity jet between the jet steam and the ice surface makes the steam move in radial direction, which assists the heat transfer around the stagnation point. The melting rate declines along the radial direction. The melting process is mainly distributed in two directions, and finally the shape of wedge is observed in the ice. In the experiment, the target ice surface is gradually moved farther away from the nozzle exit. With the progress of the jet process, melting of ice also spreads radially from the center. As the melting time increases from 106 s to 295 s, the value of melted mass increases from 67, 79 and 148 g to 251, 301 and 346 g at $V_o$ = 30, 40 and 50 m/s, respectively. The best heat transfer results, defined as slope $\frac{\Delta m}{\Delta t}$, is $V_o$ = 40 m/s in the experiment. For the velocity of 50 m/s, the intensity of heat transfer is firstly higher as the distance between jet exit and ice surface is small. The slope is small because there is a rapid increase of the distance between nozzle exit and actual ice surface. The melting rate at 50 m/s is higher at the beginning. But it decreases when the distance of steam jet exit and actual ice surface increases. For 40 m/s, the melting rate is relatively small at the beginning and gradually approaching the value of 50 m/s when the time is long enough. As the heat transfer intensity of 30 m/s is relatively weaker, from the beginning to a longer time, the melting rate is at a relatively lower level. Considering the melting time and steam velocity, the efficiency of 50 m/s is higher within 250 s, and the overall efficiency is higher for that of 40 m/s if the time is longer than 250 s.

### 5.3. Effect of number of nozzles

Fig. 6 shows the melting rate for different nozzle numbers when the boiler electric heating power is constant at 1472 W. Nozzles with one and two pipes are tested. The center-to-center spacing of the two pipe nozzles is 8 mm. Two pipes are firstly inserted into a tube with large diameter and then weld together. The external diameters of the two-pipe nozzle's pipe and one pipe nozzle are all 8 mm, with wall thickness of 1 mm. Except the difference in nozzle type, all the other experimental conditions are identical.

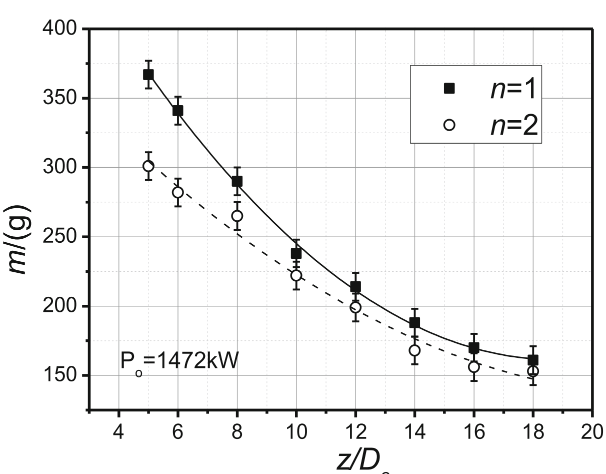


**Fig. 6.** Mass of melted ice with the effect of different nozzle number.

As shown in Fig. 6, the melting mass rate is larger for $n = 1$ than that for $n = 2$. The difference of melt between different nozzle numbers is increasing as $z/D_o$ decreases. When $z/D_o$ is larger than 8, the melting rate for two pipe nozzle is only slightly differing from that of one pipe, and the difference is mostly within 10%. As the heating power is the same, the difference is mainly in the steam pressure and flow at the exit of the nozzles. The steam pressure and velocity for the one pipe nozzle should be higher than that with two pipe nozzles. When the jet exit-to-target surface is small, the pressure in the exit should be larger for the one pipe nozzle. The jet impingement effect should be higher than the two pipe nozzle, which is beneficial for the heat transfer between the target surface and steam. When the distance increases, the jet impingement effect should decrease as the dissipation of steam to the atmosphere should not be neglected. At the non-dimensional distance more than 10, the tendency of melting rate for the two nozzle types is similar, and the decreasing rate becomes smaller. In general, for the same electrical heating power, the performance of the one pipe nozzle is relatively better than that of two pipe nozzles. The difference of melting rate at small distance is larger compared with that with larger distance.

### 5.4. Effects of nozzle diameter

Nozzle diameter is another important factor. The variation of melting rate for different nozzle diameters is shown in Fig. 7. The external diameters of 19 mm, 16 mm, 12 mm and 8 mm are tested in the experiment. Four pipes all have a tube wall thickness of 1 mm. The distance of the jet exit and initial ice surface is in the ranges of 4 to

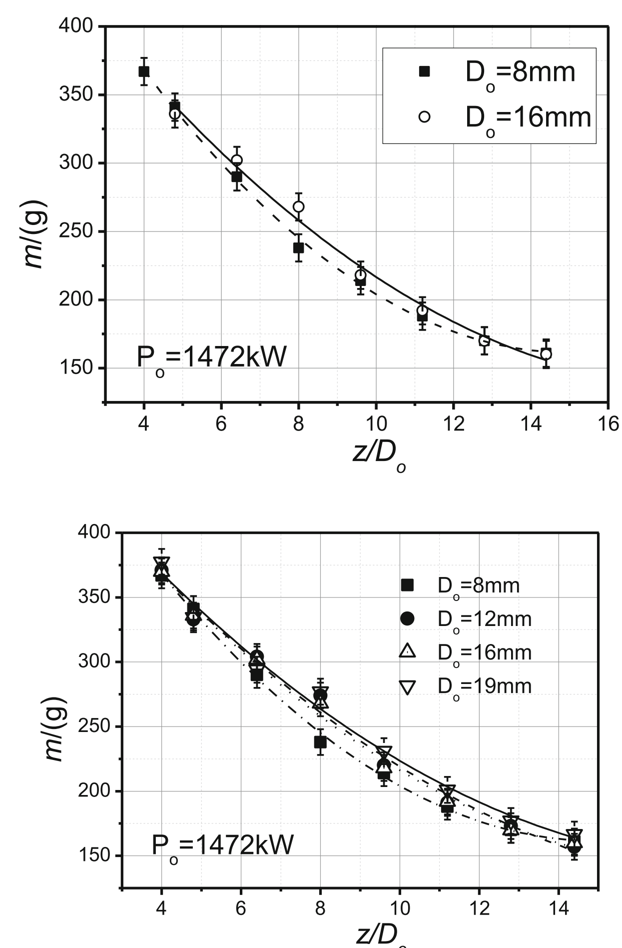


**Fig. 7.** Mass of melted ice with the effect of different nozzle outer diameters.

**Table 2**
Comparison of various deicing methods.

| Methods | Working conditions and efficiency | | | | | |
|---|---|---|---|---|---|---|
| Hot air [19] | Temperature of heat source(°C) | 30 | 40 | | 50 | 60 |
| | Energy efficiency | 9.7% | 10.2% | | 12.1% | 10.9% |
| Infrared ray [11] | Temperature of heat source(°C) | 800 | 1500 | | 2000 | |
| | Energy efficiency | 55.3% | 50.9% | | 55.9% | |
| Steam(140 °C) | Non-dimensional distances($z/D_o$) | 5 | 8 | 12 | 16 | 18 |
| | Energy efficiency | 60.5% | 46% | 34.7% | 29.2% | 27% |

14.4 cm. The jet impingement time is 225 ± 1 s. The other experimental conditions are identical. Electrical heating power of the boiler is maintained at 1472 W. As the heating power is the same, the vapor mass flow rate for different nozzle pipe diameter should be the same. The velocity of the steam should be different for the two nozzle types.

As shown in Fig. 7, the heat transfer and mass changes of the four nozzle types are almost the same within the test range. The variation might be caused by the experimental uncertainty. Such a tendency indicates that for the same boiler heating power, the ice melting characteristics for the four tube diameters are the same in the test range. In the experiment results introduced above, the dimensionless nozzle exit-to-ice surface distance $z/D_o$ is used. The effect of $D_o$ is not directly reflected. As the inner diameter of 16 mm nozzle is two times larger than that of 8 mm tube, the exit pressure of steam for the 8 mm nozzle should be higher than that of 16 mm. While the ice surface area exposed to the steam jet impingement is small for 8 mm nozzle. As the experiment progresses, the distance between jet exit and actual ice surface should be expected to increase quickly. As the increase of the distance, the melting efficiency should also decrease. The projected area is larger for the 16 mm tubes. The heat transfer might be less efficient for a specific region, but the overall efficiency is similar as that for 8 mm. Meanwhile, the increase of distance between the actual ice surface and jet exit is slower for 16 mm nozzle, it should also be beneficial for the melting rate of ice. Consequently, for a specific time, the mass of melting ice is the same for the four nozzle diameters.

For the heat transfer of steam jet impingement on the ice surface, it includes not only jet impingement processes but other processes as well, combined effect of jet impingement, steam condensing and heat conduction. As the temperature difference of steam and ice are very large, condensation heat transfer of steam outside the ice surface should not be neglected. The melts from ice should be more than the mass of condensate, because the latent heat of ice melting is considerably less than that of vaporization. As vapor condensing and ice melting outside the ice surface, a laminar film is formed outside the surface. The steam condensate and melt water flow out from the concave due to gravity. The melting ice surface will always change in the heat transfer process. With the change in the shape of ice and the disturbance of steam, the heat transfer would vary continuously along the ice surface. As indicated in [19], the melt of ice will form a layer outside the ice, which separates the melting ice and the flow jet impingement. The heat can only be conducted to the non-melting ice surface. The versatile variation tendency of the melting rate is attributed to many factors, and so far it seems still unclear in the heat transfer community. From the experiment above, the findings are mainly including the following aspects: (1) Dissipation of steam into the atmospheric environment is severe; the decreasing rate of total energy is significant as the increase of the distance between jet exit and the target ice surface. As the increases of distance, the melting rate of ice is diminishing exponentially. (2) The overall energy efficiency of steam jet impingement on ice melting is from 0.2 to 0.6. It decreases as the increase of the distance between ice surface and jet exits.

Table 2 shows the comparison of experimental result for hot air [19], infrared ray [11], and steam jet impingement method. The efficiency is defined as absorbed energy over consumed energy. The efficiency of hot air is significantly lower than the other two methods. Steam jet impingement method has the highest efficiency at the dimensionless distance of 5. The temperature of heat source for infrared ray can reach 2000 degrees Celsius in the experiment. The efficiency is normally in the range of 50%–55%. For the same power input, the melting time should be smaller for that with higher efficiency. As the fuel boiler is a relatively mature technology, the cost and occupied volume of the overall system for steam jet impingement method should be less than that for hot air and infrared ray.

The application of ice removal with the steam jet impingement method can be used for the removal of ice adhesive along electric power lines, aircraft wings, wind turbine blades, outdoor switches, and many other facilities. The experiment is conducted in an area where the ambient temperature is 10 °C and the relative humidity is about 50%. The working medium is steam. Deicing is usually used in areas or time with low temperature. In the future, experiments can be conducted in extremely cold regions where the heat loss of steam is significant. Adding salt to the water, changing to other working medium, changing the nozzle type, can also be adopted to study the performance of the steam ice removal method.

## 6. Conclusions

The heat transfer and energy efficiency of steam jet impingement on the ice surface was studied in the present study. In the experiments, the effects of non-dimensional nozzle-to-ice spacing, nozzle exit velocity, nozzle number, and nozzle diameter on heat and mass transfer were tested. Saturation temperature of steam was maintained at 140°C, dimensionless nozzle-to-ice spacing ranged from 5 to 18, and nozzle exit velocity was from 30 to 50 m/s. Based on the experimental result, it can be concluded that:

(1) The energy efficiency is increasing as the decrease of the distance between nozzle exit and ice surface. It is recommended that the dimensionless distance is controlled within 12.
(2) As the increase of jet time, the target surface moves away from the nozzle exit which made the heat transfer weakened gradually. The largest energy efficiency appeared at $V_o$ = 40 m/s.
(3) For the nozzles with one single pipe and two pipes with same external diameter, at lower dimensionless distance, one pipe nozzle has higher heat transfer performance. At the distance larger than 10, the performance is similar.
(4) The effect of nozzle diameter on heat transfer seems to be negligible for the four diameters in the investigation.

## Declaration of Competing Interest

We confirm that no conflict of interest.

## Acknowledgements

The supports from the National Science and Technology Major Project of China (2017-lll-0003-0027) and China Southern Power Grid Yunnan Power Grid Co., Ltd. are greatly acknowledged.

## References

[1] C. Ho, H. Yeh, W. Wang, J. Wang, Cool thermal discharge obtained with air flowing over melting ice by complete removal of melt, Int. Commun. Heat Mass Transf. 27 (6) (2000) 785–794.
[2] C. Ho, H. Yeh, J. Tu, Chilled air production in cool–thermal discharge systems from ice melting under constant heat flux and melt removal, Int. Commun. Heat Mass Transf. 32 (3–4) (2005) 491–500.
[3] R. Wang, L. An, P. Cao, B. Chen, M. Sysoev, D. Fan, P.G. Talalay, Rapid ice drilling with continual air transport of cuttings and cores: general concept, Polar Sci. 14

(2017) 21–29.
[4] E. Heucke, A light portable steam-driven ice drill suitable for drilling holes in ice and firn, Geografiska Annaler: series a, Phys. Geogr. 81 (4) (1999) 603–609.
[5] S.M. Hodge, Instruments and methods: a new version of a steam-operated ice drill, J. Glaciol. 10 (60) (1971) 387–393.
[6] F.J.J.o.G. Howorka, Instruments and methods: a steam-operated ice drill for the installation of ablation stakes on glaciers, J. Glaciol. 5 (41) (1965) 749–750.
[7] P. Talalay, Perspectives for development of ice-core drilling technology: a discussion, Ann. Glaciol. 55 (68) (2014) 339–350.
[8] D.S. Chavan, R. Pal, J. Sankpal, V. Sahil, A. Singh, B.S. Gadhwal, Ice removal from wind turbine using hot water flow through blade, 2017 International Conference on Energy, Communication, Data Analytics and Soft Computing (ICECDS), IEEE, 2017, pp. 870–875.
[9] Anonymous author, Hot water drilling in Antarctic ice, World Pumps 6 (2012) 32–35.
[10] P. Ratanadecho, K. Aoki, M. Akahori, A numerical and experimental investigation of the modelling of microwave melting of frozen packed beds using a rectangular wave guide, Int. Commun. Heat Mass Transf. 28 (6) (2001) 751–762.
[11] T. Xie, J. Dong, H. Chen, Y. Jiang, Y.J.E. Yao, Experiment investigation on deicing characteristics and energy efficiency using infrared ray as heat source, Energy 116 (pt.1) (2016) 998–1005.
[12] N. Seki, M. Sugawara, S.J.W.-U.S. Fukusako, Radiative melting of ice layer adhering to a vertical surface, Wärme-und Stoffübertragung 12 (2) (1979) 137–144.
[13] N. Seki, M. Sugawara, S.J.W.-U.S. Fukusako, Radiative melting of a horizontal clear ice layer, Wärme-und Stoffübertragung 11 (3) (1978) 207–216.
[14] S. Thongwik, T. Kiatsiriroat, A. Nuntaphan, Heat transfer model of slurry ice melting on external surface of helical coil, Int. Commun. Heat Mass Transf. 35 (10) (2008) 1335–1339.
[15] W.H. Sang, Y.T. Lee, J.D. Chung, S.T. Kim, T. Kim, C.-H. Oh, K.-H. Lee, Efficient numerical approach for simulating a full scale vertical ice-on-coil type latent thermal storage tank, Int. Commun. Heat Mass Transf. 78 (2016) 29–38.
[16] P.R. Chakraborty, Enthalpy porosity model for melting and solidification of pure-substances with large difference in phase specific heats, Int. Commun. Heat Mass Transf. 81 (2017) 183–189.
[17] H.A. Hamzeh, M. Miansari, Numerical study of tube arrangement and fin effects on improving the ice formation in ice-on-coil thermal storage systems, Int. Commun. Heat Mass Transf. 113 (2020) 104520.
[18] G.G. Koenig, C.C. Ryerson, An investigation of infrared deicing through experimentation, Cold Reg. Sci. Technol. 65 (2011) 79–87.
[19] T. Xie, J. Dong, H. Chen, Y. Jiang, Y. Yao, Experimental investigation of deicing characteristics using hot air as heat source, Appl. Therm. Eng. 107 (2016) 681–688.
[20] J. Burnett, F.R. Rack, D. Blythe, P. Swanson, D. Duling, D. Gibson, C. Carpenter, G. Roberts, J. Lemery, S. Fischbein, Developing a hot-water drill system for the WISSARD project: 3. Instrumentation and control systems, Ann. Glaciol. 55 (2014) 303–310.
[21] D.S. Blythe, D.V. Duling, D.E. Gibson, Developing a hot-water drill system for the WISSARD project: 2. In situ water production, Ann. Glaciol. 55 (68) (2014) 298–302.
[22] F.R. Rack, Enabling clean access into subglacial Lake Whillans: development and use of the WISSARD hot water drill system, P. Roy. Soc. A-Math. Phy. 374 (2016) 20140305.
[24] K. Makinson, D. Pearce, D.A. Hodgson, M.J. Bentley, A.M. Smith, M. Tranter, M. Rose, N. Ross, M. Mowlem, J. Parnell, Clean subglacial access: prospects for future deep hot-water drilling, P. Roy. Soc. A-Math. Phy. 374 (2016) 20140304.
[25] G. Liu, P. Talalay, R. Wang, Y. Yang, J. Hong, D. Gong, A. Liu, D. Fan, Design parameters of hot-water drilling systems, Water 11 (2019) 289.
[26] P. Talalay, G. Liu, R. Wang, X. Fan, J. Hong, D. Gong, B. Liu, A. Liu, S. Mihail, Shallow hot-water ice drill: estimation of drilling parameters and testing, Cold Reg. Sci. Technol. 155 (2018) 11–19.
[27] P. Talalay, B. Liu, Y. Yang, X. Fan, J. Hong, D. Gong, M. Sysoev, X. Li, Y. Li, Electric thermal drills for open-hole coring in ice, Polar Sci. 17 (2018) 13–22.
[28] F. Masuda, T. Nakatogawa, K. Kawanishi, M. Isono, Experimental study on an impingement high-pressure steam jet, Nucl. Eng. Des. 67 (2) (1982) 273–286.
[29] F.H.T. Moody, Maximum flow rate of a single component, two-phase mixture, J. Heat Transf. 87 (1) (1965) 134.
[30] M. Yamada, M. Okada, Enhancement of the melting of an ice cylinder by the combination with the condensation of a saturated steam flow, J. Therm. Sci. Technol. 6 (2011) 43–56.
[31] D.C. Woodcock, J.S. Gilbert, S.J. Lane, Ice-melt rates by steam condensation during explosive subglacial eruptions, J. Geophys. Res-Sol. Ea. 120 (2015) 864–878.
[35] R.J. Moffat, Using uncertainty analysis in the planning of an experiment, J. Fluids Eng. 107 (1985) 173–178.
[36] J. Stevens, B. Webb, Measurements of flow structure in the stagnation zone of impinging free-surface liquid jets, Int. J. Heat Mass Transf. 36 (1993) 4283–4286.

## Nomenclature

$D_o$: outer diameter of nozzle pipe($mm$)
*I:* current of electric heater(A)
*m:* mass of melting ice(kg)
$m_1$: mass of ice container before melting(kg)
$m_2$: mass of ice container after the jet impingement(kg)
*n:* number of pipes for the nozzle
*U:* voltage of electric heater(V)
$P_t$: energy absorbed by ice($W$)
$P_0$: electric heating power($W$)
*r:* latent heat of vaporization ($J/kg$)
*R:* radial distance($mm$)
*t:* steam jet impingement time($s$)
$T_w$: initial temperature of ice surface($^\circ C$)
$T_{l,\ sat}$: saturation temperature of liquid water in the boiler ($^\circ C$)
$T_{s,\ sat}$: temperature of steam in the boiler ($^\circ C$)
$T_j$: steam jet temperature ($^\circ C$)
$V_o$: nozzle exit steam velocity(m/s)
*V:* velocity of steam(m/s)
*z:* initial nozzle-to-ice spacing ($mm$)
$\gamma$: energy efficiency
*RTDs:* resistance temperature detectors
*x:* hose length ($m$)